H_∞ DESIGN OF ROTOR FLUX ORIENTED CONTROLLED INDUCTION MOTOR DRIVES: SPEED CONTROL, STABILITY ROBUSTNESS AND NOISE ATTENUATION

João C. Basilio[1,†], José A. Silva Jr.[2,††], Jr., and Luis G. B. Rolim[3], Member, IEEE

[1,3]DEE, UFRJ, Cidade Universitária, Rio de Janeiro, Brazil, e-mail : basilio[1],rolim[3]@dee.ufrj.br
[2]COPPE, UFRJ, Cidade Universitária, Rio de Janeiro, Brazil, e-mail: alencar@pee.coppe.ufrj.br

***Abstract*— In this paper the design of a control system for rotor flux oriented controlled induction motor drives using H_∞ optimal control theory is carried out. Two H_∞ problems are considered: *(i)* a 1-block problem with the view to maximizing the system performance; *(ii)* a 2-block problem with the weights initially chosen for maximizing both the system performance (transient response) and the system tolerance to uncertainty in the plant model (robust performance), and in the sequel the weights are modified to account for transient performance and noise attenuation. All the designed controllers have been implemented in a real system, and the results are shown in the paper.**

KEYWORDS

Vector control, H_∞ control theory, optimal control, feedback system.

I. INTRODUCTION

Rotor flux oriented controlled induction motor drives have recently received great attention in the literature [1], [2], and the references therein. This has led to the so-called vector control method which is based on the transformation of the nonlinear model of the induction motor in a linear time-invariant first order model. In order to obtain an exact first order model, it is necessary to pre-multiply the system by a matrix whose elements are functions of the rotor flux angle. However, this angle is not known exactly, being estimated from the rotor time constant (the ratio between the rotor inductance and resistance), and the shaft velocity. Since, up to now, there is no reliable method for the exact determination of the rotor time constant, the transformation does not lead to an exact first order model.

The difference between the exact first order model (which in this paper will be referred to as the nominal model) and the real model can be seen as a model uncertainty. This suggests that robust design techniques can be employed to obtain a controller for this system. One of the design techniques that can be used is the so-called H_∞ optimal control theory [3], [4]. This approach has been deployed in previous works, [5], [6], in which 2-block H_∞ problems have been formulated and solved using the so-called DGKF approach [7]. The main difference between these works is the choice of weights: in [5], scalar weights have been used while in [6], although stable rational functions have been used as weights, they have been chosen according to H_∞ dogmas, *i.e.* the weight for robustness is a high pass function, as prescribed in the H_∞ theory, without checking if this is what actually happens when the estimated rotor time constant is supposed to be different from the real one.

† Partially supported by CNPq
†† Partially supported by CAPES

In this paper two H_∞ problems are considered: *(i)* a 1-block problem, with the view to maximizing the system performance (assuming the shaft velocity as the variable to be controlled); *(ii)* a 2-block problem with the weights initially chosen for maximizing both the system performance (transient response) and the system tolerance to uncertainty in the plant model (robust performance), and, in the sequel, the weights are modified to account for transient performance and noise attenuation. Differently from [5], [6], the solution here is obtained following the standard 1984 approach [4], [8]. The main advantage of using such an approach over DGKF solution is that the designer has a clear view on how to change the weights in order to improve the control objectives. Furthermore, the use of 1984 approach has led to an interesting result: the H_∞ controller, solution to the 1-block problem is a PI controller, whose parameters are tuned according to the so-called internal model control [9]. This unexpected result justifies, from the H_∞ theory point of view, why PI controllers have been successfully used in field oriented control of induction motors. Another point which differs this paper from [6], is that here the weight for robustness is obtained from frequency response experiments carried out in the real system by perturbing the estimated rotor time constant.

It is well known that the objectives of robustness and noise attenuation are expressed in terms of the same 2-block H_∞ optimization problem; the only difference is that the weight must now be a high pass rational function. This problem has also been tackled in this paper, and the results obtained from practical implementation are shown.

II. A LINEAR MODEL FOR ROTOR FLUX ORIENTED CONTROL OF CURRENT-FED INDUCTION MOTORS

A. Theoretical background

Assuming as inputs, the stator current vector components in field coordinates, $i_{Sd}(t)$ (the stator current component in the direction of the magnetising current vector, usually referred to as the direct component) and $i_{Sq}(t)$ (the quadrature component of the stator current, which is perpendicular to $i_{Sd}(t)$), then current-fed induction motors can be modeled as [1]:

$$\begin{cases} T_R \dfrac{d}{dt} i_{mR}(t) + i_{mR}(t) = i_{Sd}(t) \\ \dfrac{d}{dt}\rho(t) = \omega(t) + \dfrac{i_{Sq}(t)}{T_R i_{mR}(t)} \\ J\dfrac{d}{dt}\omega(t) + f\omega(t) = k i_{mR}(t) i_{Sq}(t) \\ \omega(t) = \dfrac{d}{dt}\varepsilon(t) \end{cases} \quad (1)$$

where $T_R = L_R/R_R$ denotes the rotor time constant, L_R

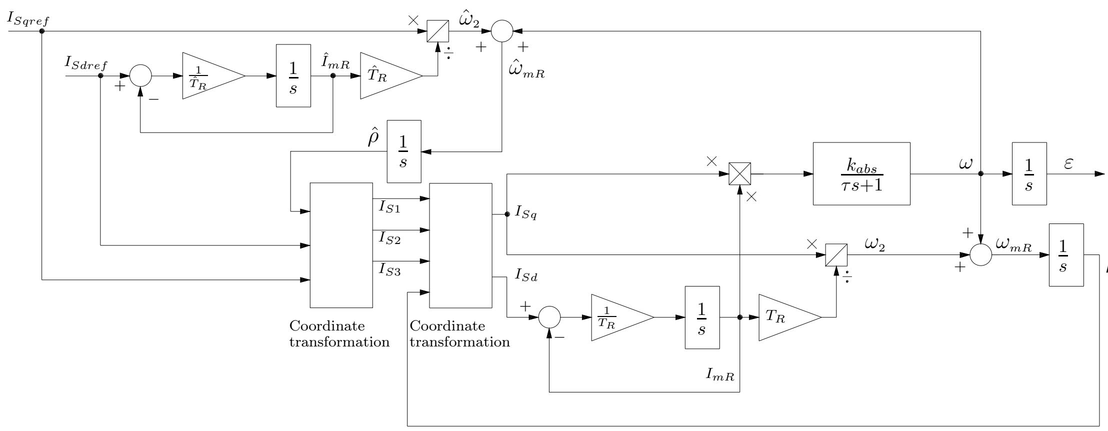

Fig. 1. Block diagram of an ideal inverter in cascade with a current fed induction motor, and with a rotor flux angle estimator.

and R_R are, respectively, the rotor inductance and resistance, $i_{mR}(t)$ is the magnetising current, $\rho(t)$ is the rotor flux angle with respect to the stator axis, J is the motor inertia, f is the viscous friction, $\omega(t)$ is the instantaneous angular velocity of the rotor, k is the coupling factor, which is a function of the total leakage factor of the motor and of the stator inductance, and $\varepsilon(t)$ the angle of rotation of the rotor, measured in the stator frame of coordinates. Notice that, if in Eqs. (1), the direct component of the stator current is made constant, *i.e.*, $i_{Sd}(t) = I_{Sd}$, then, after a brief transient, which is dictated by the rotor time constant T_R, $i_{mR}(t)$ becomes equal to I_{Sd}. When this happens, the electrical torque becomes a function of $i_{Sq}(t)$, only, and, thus, the model of a current-fed induction motor becomes analogous to that of a constant field dc-motor controlled by the armature current. However, $i_{Sq}(t)$ and $i_{Sd}(t)$, are not accessible; they are actually functions of the line currents $i_{S1}(t)$, $i_{S2}(t)$ and $i_{S3}(t)$, as follows:

$$\begin{bmatrix} i_{Sd}(t) \\ i_{Sq}(t) \end{bmatrix} = \begin{bmatrix} \frac{3}{2}\cos\rho(t) & \frac{\sqrt{3}}{2}\sin\rho(t) & -\frac{\sqrt{3}}{2}\sin\rho(t) \\ -\frac{3}{2}\sin\rho(t) & \frac{\sqrt{3}}{2}\cos\rho(t) & -\frac{\sqrt{3}}{2}\cos\rho(t) \end{bmatrix} \begin{bmatrix} i_{S1}(t) \\ i_{S2}(t) \\ i_{S3}(t) \end{bmatrix}. \tag{2}$$

Therefore, in order to have as inputs the direct and quadrature components of the stator current, one has to carry out an inverse transformation of Eq. (2), given as:

$$\begin{bmatrix} i_{S1}(t) \\ i_{S2}(t) \\ i_{S3}(t) \end{bmatrix} = \begin{bmatrix} \frac{2}{3}\cos\rho(t) & -\frac{2}{3}\sin\rho(t) \\ \frac{\sqrt{3}}{3}\sin\rho(t) & \frac{\sqrt{3}}{3}\cos\rho(t) \\ -\frac{\sqrt{3}}{3}\sin\rho(t) & -\frac{\sqrt{3}}{3}\cos\rho(t) \end{bmatrix} \begin{bmatrix} i_{Sd}(t) \\ i_{Sq}(t) \end{bmatrix}. \tag{3}$$

The device which causes the motor currents to follow the references given in (3) is called a current-controller PWM inverter (in this work it will be simply referred to as inverter). It is clear from Eq. (3) that the inverter inputs are the desired values for the direct and quadrature components of the stator current, here denoted as $i_{Sdref}(t)$ and $i_{Sqref}(t)$ and as outputs the line currents $i_{S1}(t)$, $i_{S2}(t)$ and $i_{S3}(t)$ necessary to make $i_{Sd}(t)$ and $i_{Sq}(t)$ (the actual values) equal their reference values.

Assuming $i_{Sdref}(t) = I_{Sdref}$ (constant), then the transfer function for the system formed with an ideal inverter and a current-fed induction motor which relates $i_{Sqref}(t)$ and $\omega(t)$ is given by:

$$G(s) = \frac{\Omega(s)}{I_{Sqref}(s)} = \frac{kI_{Sdref}}{Js+f} = \frac{k_{abs}I_{Sdref}}{\tau s+1} \tag{4}$$

where $\tau = J/f$ and $k_{abs} = k/f$.

Although appealing from the theoretical point of view, this approach has the following drawback: since the rotor flux angle $\rho(t)$ cannot be measured, it should be estimated. However, as shown in Fig. 1, its estimate depends on the knowledge of the rotor time constant T_R, whose value cannot be determined precisely. If by chance the value of the estimated rotor time constant $\hat{T}_R$ is exactly equal to T_R then the behavior of the system estimator+inverter+induction motor can be described by Eq. (4). However, in general $\hat{T}_R \neq T_R$, and thus Eq. (4) is no longer a reliable model for the system. One way of taking into account model uncertainty is to use, instead of the transfer function given in Eq. (4), a so-called perturbed transfer function $G_P(s)$. In this work, multiplicative unstructured perturbation [10] will be used, which is given by:

$$G_P(s) = [1 + W_1(s)]G(s), \tag{5}$$

where $W_1(s)$ is a stable transfer function and will be determined from frequency response experiments carried out at the real system by perturbing $\hat{T}_R$. This provides the necessary information for dealing with controller design within the H_∞ control theory.

B. *Parameter identification and model validation*

The motor used to validate the theory presented in this paper is a class A three-phase two-pole Δ-connected induction motor with squirrel-cage rotor. Its nominal values are: *(i)* Power: $60W$; *(ii)* Line voltage: $30V$, *(iii)* Frequency: $60Hz$; *(iv)* Line current: $2.8A$ and *(v)* Rotor inertia: $J = 0.00057Kg.m^2$.

According to the model given in Fig. 1, the only parameters to be determined are T_R, k_{abs} and τ. Let us consider, initially, the identification of T_R. An immediate choice for the estimated value of T_R ($\hat{T}_R$) is that obtained by performing standard tests for determining the steady-state circuit model parameters [11]. For the induction motor used in this work, it has been obtained $\hat{T}_R = 0.0519s$. A better estimation for the rotor time constant can be obtained if we notice that the system inverter+estimator+induction motor only behaves as

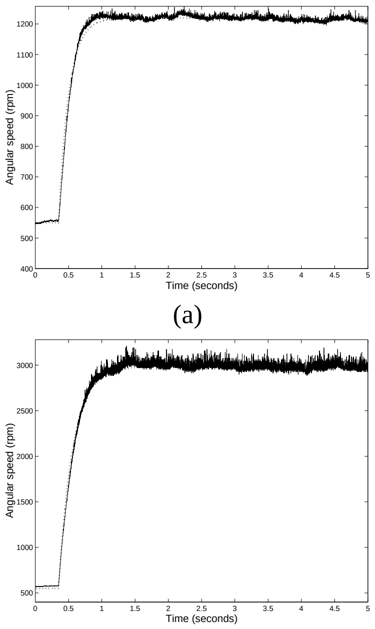

(a)

(b)

Fig. 2. Step responses for the real system (solid lines) and for the Simulink model (dotted lines).

and ideal first order one when $\hat{T}_R$ is exactly equal T_R (the actual value of the rotor time constant). A better estimation of T_R can then be obtained by trial-and-error, *i.e.*, by changing the value of $\hat{T}_R$ in the real estimator until the system response to an step input matches that of a first order one. This has actually been done in this work, leading to a value of $\hat{T}_R$ approximately 5% smaller than that obtained previously, *i.e.* $\hat{T}_R = 0.0493s$. Consider, now, the estimation of k_{abs} and τ. Since the value of $\hat{T}_R$ is such that the system now behaves as a first order one, usual tests for estimation of the parameters of first order systems can be deployed to find k_{abs} and τ. Among the available techniques, the so-called Method of Area [12] seems more appropriate due to the noise introduced in the system response by the sensor. At this point, it is worth remarking that, before applying a step signal in $i_{Sqref}(t)$, it is necessary to apply a constant input to $i_{Sdref}(t)$, *i.e.*, $i_{Sdref}(t) = I_{Sdref}$. For the experiments carried out in this work, it has been adopted $I_{Sdref} = 2.8A$. Finally, average values for k_{abs} and τ have been obtained after performing these experiments for several step signals with different amplitudes, leading to $k_{abs} = 14.7287$ and $\tau = 0.2030$.

Fig. 2 shows the comparisons between the simulation results (dotted lines) and those obtained experimentally (solid lines) by applying to a Simulink model, equivalent to the block diagram of Fig. 1 (with the above estimated values of $\hat{T}_R$, k_{abs} and $T_R = \hat{T}_R$), and to the real system step signals of amplitudes $3.2246A$ (Fig. 2.a) and $7.2999A$ (Fig. 2.b). It is worth remarking that in both cases, steps of amplitude $1.5802A$ were initially applied to $i_{Sqref}(t)$ and that $I_{Sdref} = 2.8A$.

III. CHARACTERIZATION OF CONTROL OBJECTIVES IN TERMS OF THE MINIMIZATION OF H_∞ NORMS OF TRANSFER FUNCTIONS

Consider the block diagram of Fig. 3 where $r(s)$, $e(s)$, $d(s)$, $y(s)$ and $\eta(s)$ denote, respectively, the Laplace trans-

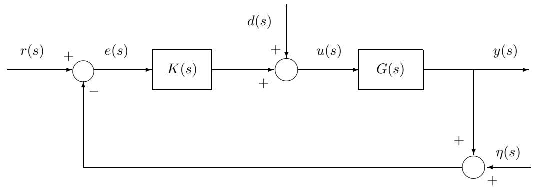

Fig. 3. Block diagram of a standard negative unit feedback system.

forms of the reference, error, external disturbance, output and sensor noise signals, and $G(s)$ and $K(s)$ are the transfer functions of the plant and the controller, respectively. Stability robustness (or system tolerance to plant uncertainty), tracking of square integrable reference signals, transient performance, external disturbance rejection and noise attenuation are usual control objectives and can be expressed in terms of the minimization of the H_∞ norms of transfer functions[1] as follows:

1. Robust stability:
$$\min_{\text{Stabilizing } K(s)} \|W_1 T\|_\infty, \tag{6}$$
where $W_1(s)$ is a stable rational weighting function defined according to Eq. (5) and $T(s) = G(s)K(s)[1 + G(s)K(s)]^{-1}$ is the transfer function between $r(s)$ and $y(s)$.
2. Tracking of square integrable reference signal and transient performance:
$$\min_{\text{Stabilizing} K(s)} \|W_2 S\|_\infty, \tag{7}$$
where $W_2(s)$ is a stable rational weighting function used to place more penalty on the relevant frequencies and $S(s) = [1 + G(s)K(s)]^{-1} = 1 - T(s)$ is the well known sensitivity function.
3. Rejection of square integrable external disturbance signal:
$$\min_{\text{Stabilizing } K(s)} \|W_3 SG\|_\infty. \tag{8}$$
4. Noise attenuation:
$$\min_{\text{Stabilizing } K(s)} \|W_4 T\|_\infty. \tag{9}$$
where $W_4(s)$ is a stable rational weighting function used to place more penalty on the noise dominant frequencies.

H_∞ optimization problems can also be formulated to take into account two or more control objectives; for example, robust stability and tracking or noise attenuation and tracking can be addressed simultaneously, as follows:
$$\min_{\text{Stabilizing } K(s)} \left\| \begin{array}{c} W_i T \\ W_2 S \end{array} \right\|_\infty, \tag{10}$$
where $i = 1$ for robust stability and $i = 4$ for noise attenuation. It is important to remark that since $T(s) + S(s) = 1$, then control objectives addressed in Eq. (10) are conflicting, in the sense that it is not possible to have at the same time stability robustness and transient performance. The only exception is when the weighting functions $W_1(s)$, $W_2(s)$ and $W_4(s)$ place more penalty on different frequencies, as follows: *(i)* in linear systems, frequency response identification usually leads to more imprecise description at high frequencies, and thus, in this case, $W_1(s)$ must be a high pass transfer function; *(ii)* signals to be tracked have usually a pre-defined frequency, and thus, $W_2(s)$ must be a low pass transfer function; *(iii)* finally,

[1]The H_∞-norm of a stable transfer function $H(s)$ is defined as $\|H\|_\infty = \max_{\omega \in \mathbb{R}_+} |H(jw)|$, where $|.|$ denotes absolute value.

sensor noises have usually high frequency components, which implies that $W_4(s)$ must also be a high pass transfer function.

In order to obtain the solutions of H_∞ optimization problems posed above, the first step is to guarantee that the resulting controller stabilizes the nominal transfer function. This is done through the so-called Youla-Kucera parametrization, in which the controller is parametrized in terms of a stable and proper rational transfer function[2] $Q(s)$ as follows:

$$K(s) = -\frac{Y(s) - M(s)Q(s)}{X(s) - N(s)Q(s)} \qquad (11)$$

where $N(s)$, $M(s)$, $X(s)$ and $Y(s)$ are stable rational functions such that

$$G(s) = \frac{N(s)}{M(s)} \qquad (12)$$

and satisfy the Bezout equation

$$X(s)M(s) + Y(s)N(s) = 1. \qquad (13)$$

It can be shown [4] that all the optimization problems described by Eqs. (6) to (10) can be transformed into the following problem

$$\min_{Q(s)\in RH_\infty} \|T_1 - T_2 Q\|_\infty, \qquad (14)$$

where $T_1(s)$ and $T_2(s)$ are rational functions and depend on the optimization problem which is being considered. This optimization problem is usually referred to, in the literature, as a model matching problem [4].

IV. A 1-BLOCK H_∞ CONTROLLER FOR SPEED CONTROL

A. Problem formulation and main results

The control problem to be considered initially has a unique control objective, *i.e.* tracking and transient performance of a reference signal, which in this case is the rotor angular velocity. Within the H_∞ framework, this control object leads to the optimization problem given by Eq. (7). Therefore, using the Youla-Kucera parametrization (11) in Eq. (7), and after some straightforward calculation, one may write:

$$\min_{\text{Stabilizing } K(s)} \|W_2 S\|_\infty = \min_{Q(s)\in RH_\infty} \|W_2(X - NQ)M\|_\infty$$

$$= \min_{Q(s)\in RH_\infty} \|T_1 - T_2 Q\|_\infty, \qquad (15)$$

where, in this case, $T_1(s) = W_2(s)X(s)M(s)$ and $T_2(s) = W_2(s)N(s)M(s)$. Notice that, since the plant transfer function (4) is already stable, then an immediate choice for $N(s)$ and $M(s)$ which satisfy Eq. (12) is given as:

$$N(s) = G(s) \text{ and } M(s) = 1. \qquad (16)$$

It is therefore easy to see that $X(s)$ and $Y(s)$ solutions to Eq. (13) will be given by:

$$X(s) = 1 \text{ and } Y(s) = 0. \qquad (17)$$

Thus, it is not hard to see that the solution to the optimization problem (15) is trivial and independent of $W_2(s)$, being given by:

$$Q(s) = \frac{1}{G(s)} = \frac{\tau s + 1}{k_{abs} I_{Sdref}}. \qquad (18)$$

However this solution is improper and, therefore, does not satisfy the requirement that $Q(s) \in RH_\infty$. In order to circumvent this problem, what is usually done [13] is to approximate

[2]Such a function is usually referred to as an RH_∞ function or to belong to RH_∞.

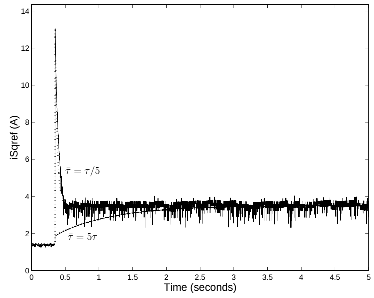

(a)

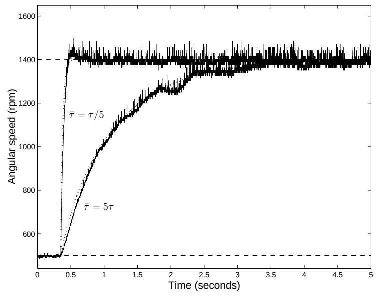

(b)

Fig. 4. Closed loop response for a step reference signal of $1400rpm$ (a) and control signal $i_{Sqref}(t)$ (b) obtained from the real system (solid lines) and by simulation (dotted lines).

this function by a rational one. This is carried out by introducing a polynomial factor $\bar\tau s + 1$ on the denominator polynomial of $Q(s)$, *i.e.*

$$Q_P(s) = \frac{1}{\bar\tau s + 1} Q(s) = \frac{\tau s + 1}{k_{abs} I_{Sdref}(\bar\tau s + 1)} \qquad (19)$$

where $\bar\tau$ is chosen with the view to approximating $Q_P(s)$ and $Q(s)$ at the frequency range of interest. Direct substitution of $N(s)$, $M(s)$, $X(s)$, $Y(s)$ and $Q_P(s)$ given by Eqs. (16), (17) and (19) in the controller expression (11) and after some straightforward calculation, results in:

$$K(s) = \frac{\tau}{k_{abs} I_{sdref} \bar\tau} \frac{\tau s + 1}{s} = K_p \left(1 + \frac{1}{T_i s}\right) \qquad (20)$$

where

$$K_p = \frac{\tau}{k_{abs} I_{sdref} \bar\tau} \text{ and } T_i = \tau. \qquad (21)$$

Eq. (20) above shows that the H_∞ controller which optimizes tracking and transient performance is a PI controller whose parameters are tuned according to the so-called internal model principle applied to PID controllers [9]. This is an amazing result and explains, from the H_∞ point of view, why PI controllers have been used successfully in vector control. Another important contribution of this result is that it presents the correct way of tuning the PI controller, as shown in Eq. (21). Furthermore, notice from Eq. (21), that the proportional gain K_p increases when $\bar\tau$ decreases. The importance of this fact is that it does not contradict the control system theory for which the increase in the gain is used to speed up the system response and the H_∞ control theory, for which the best controller for performance is obtained when $\bar\tau$ approaches zero.

B. Experimental results

With the view to showing the validity of the theoretical results presented in this section, two real H_∞ PI controllers have been used to control the rotor velocity of the real induction motor whose parameters are given in Subsection II-B. In all experiments, $I_{Sdref} = 2.8A$, and thus, according to Eq. (21), the controller parameters must be tuned as:

$$K_p = \frac{0.0049223}{\bar{\tau}} \text{ and } T_i = 0.2030. \tag{22}$$

Experimental results are shown in Fig. 4 for $\bar{\tau} = 5\tau$ and $\bar{\tau} = \tau/5$. Fig. 4(a) shows the rotor speed for a step reference signal of $1400rpm$ and Fig. 4(b) shows the behavior of the quadrature component of the stator current; the solid lines have been acquired from the real system while the dotted lines have been obtained from simulation. Notice that the response rise time and settling time have decreased, respectively, from approximately $1.39s$ and $3.15s$ for $\bar{\tau} = 5\tau$ to $50ms$ and $40ms$ for $\bar{\tau} = \tau/5$, producing the expected results.

V. 2-BLOCK H_∞ CONTROLLERS

According to Eq. (10) when other control objectives, such as robust stability or noise attenuation, are to be considered in addition to system performance, it is necessary to formulate a 2-block H_∞ problem. Furthermore, substituting Eq. (11) in (10), the following problem, equivalent to that given in (10) is obtained:

$$\min_{Q(s)\in RH_\infty} \left\| \begin{bmatrix} -W_i Y\tilde{N} \\ W_2 X\tilde{M} \end{bmatrix} - \begin{bmatrix} -W_i N \\ W_2 N \end{bmatrix} \tilde{M}Q \right\|_\infty \tag{23}$$

where $i = 1$ for robust stability and $i = 4$ for noise attenuation. Defining

$$T_1(s) = \begin{bmatrix} -W_i Y\tilde{N} \\ W_2 X\tilde{M} \end{bmatrix} \text{ and } T_2(s) = \begin{bmatrix} -W_i N \\ W_2 N \end{bmatrix} \tilde{M} \tag{24}$$

then Eq. (23) is equivalent to:

$$\min_{Q(s)\in RH_\infty} \|T_1 - T_2 Q\|_\infty. \tag{25}$$

As pointed out in Section III, the weighting functions $W_2(s)$ and $W_4(s)$ should be, respectively, low and high pass transfer functions, and are chosen by the designer in order to place more penalty at the desired frequencies. On the other hand, weight $W_1(s)$ takes into account uncertainties on the mathematical model and, for this reason, should be obtained experimentally; this will be the subject of the next subsection. In both cases, first order weights will be deployed, having, therefore, the following transfer functions

$$W_i(s) = \frac{a_i(s+b_i)}{(s+c_i)} \text{ and } W_2(s) = \frac{a_2(s+b_2)}{(s+c_2)} \tag{26}$$

where $a_i, b_i, c_i > 0$, $i = 1, 4$, $b_2 > c_2$ and $b_4 < c_4$. The relationship between b_1 and c_1 will be defined from frequency response experiments. Expressions for $T_1(s)$ and $T_2(s)$ can be obtained by substitution of Eqs. (16), (17) and (26) in (24), being given as:

$$T_1(s) = \begin{bmatrix} 0 \\ \dfrac{a_2(s+b_2)}{(s+c_2)} \end{bmatrix}, T_2(s) = \begin{bmatrix} -\dfrac{a_i(s+b_i)}{(s+c_i)} \\ \dfrac{a_2(s+b_2)}{(s+c_2)} \end{bmatrix} \frac{k_{abs} I_{Sdref}}{\tau s + 1}. \tag{27}$$

Differently from the 1-block problem, it is not possible to obtain here a closed solution. It is well known that the solution for the 2-block H_∞ problem is obtained by iterative methods. The readers are referred to [4] for more details on the solution of problem (23) for $T_1(s)$ and $T_2(s)$ given by Eq. (27).

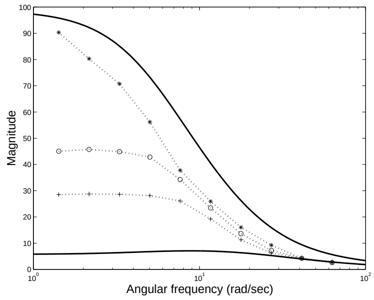

Fig. 5. Experimental results obtained for $\hat{T}_R = 0.0493s$ ($\cdot o \cdot$) and by perturbing $\hat{T}_R$ in $+50\%$ ($\cdot o \cdot$) and -50% ($\cdot \star \cdot$) and $|G(j\omega)||1 \pm W_1(j\omega)|$ (solid lines).

A. *Influence of the inexact knowledge of the rotor time constant on the induction motor linear model*

As point out in Subsection II-A the inexact knowledge of the rotor time constant will be considered as a model uncertainty. In this work it has been used the so-called model with multiplicative perturbation given in Eq. (5). It is clear from Eq. (5) that, for each frequency ω_k

$$\frac{G_P(j\omega_k)}{G(j\omega_k)} - 1 = W_1(j\omega_k) \tag{28}$$

and, thus, it is straightforward to see that

$$\left|\frac{G_P(j\omega_k)}{G(j\omega_k)} - 1\right| \le |W_1(j\omega_k)| \le \left|\frac{G_P(j\omega_k)}{G(j\omega_k)} + 1\right|. \tag{29}$$

It is worth noting that $G(j\omega_k)$ will be obtained for $\hat{T}_R$ nominal while $G_P(j\omega_k)$ will be obtained from the system frequency response by perturbing $\hat{T}_R$. Fig. 5 shows the results obtained experimentally by perturbing $\hat{T}_R$ in $+50\%$ (cross-dotted line) and -50% (star-dotted line). From these data, a first order weight, defined according to Eq. (26), is given by:

$$W_1(s) = \frac{0.2(s+131)}{s+23}. \tag{30}$$

Notice that, this weight satisfies Eq. (29) for each ω_k, as can be shown in Fig. 5 (solid lines). Furthermore, it is clear that the rational function given by Eq. (30) places more penalty at low than at high frequencies. This contradicts the usual assumption of H_∞ control theory that $W_1(s)$ should be a high pass transfer function. Therefore, the weight used in [6] to address robustness bears no relationship with practice, since it has been chosen as a high pass transfer function. The main implication of the weight given in (30) is the fact that both weights $W_1(s)$ and $W_2(s)$ place penalty at the same frequency range (low frequencies) and thus the 2-block H_∞ problem cannot be used to improve robustness without severe degradation on system performance.

B. *2-block H_∞ controller for transient performance and noise attenuation*

Consider again the minimization problem given in Eq. (24) for $i = 4$, *i.e.*, with the objective of noise attenuation at the plant output being incorporated to the controller design. It is important to remark that since the tachometer is the main source of noise, then the measure of the noise attenuation at the plant output will be made in an indirect way, namely, through the measure of the plant input signal, which in the present work is $i_{Sqref}(t)$.

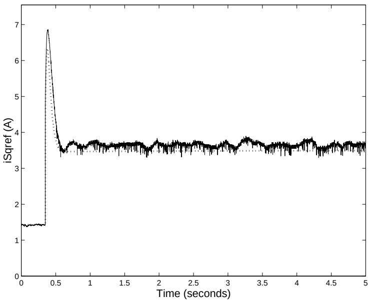

(a)

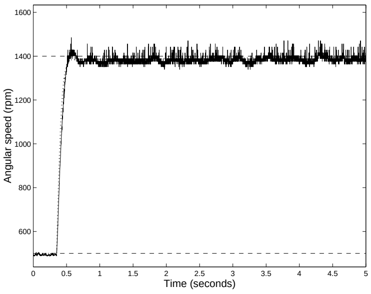

(b)

Fig. 6. Closed loop response for a step reference signal of $1400rpm$ (a) and control signal $i_{Sqref}(t)$ (b) obtained from the real system (solid lines) and by simulation (dotted lines) for the 2-block H_∞ controller

An important step in the design of H_∞ controller is the choice of weights. Although the designer knows what their frequency responses should look like, better weights are chosen in a trial-and-error bases. Indeed, using as weights

$$W_4(s) = \frac{s+30}{s+100} \text{ and } W_2(s) = \frac{0.1(s+1)}{s+0.01}, \qquad (31)$$

then the following H_∞ controller has been obtained:

$$K(s) = \frac{0.0345(s+10)(s+5.7477)(s+0.3229)}{(s+49.2995)(s+0.6664)(s+0.0072)}. \qquad (32)$$

The system closed-loop response for a step reference signal is shown in Fig. 6(b) and the corresponding control signal ($i_{Sqref}(t)$) is shown in Fig. 6(a). Notice that the rise time is now $90ms$ and the settling time $530ms$, approximately, which is slightly worse than the corresponding performance indexes for the 1-block H_∞ controller for $\bar{\tau} = \tau/5$, whose response is shown in Fig. 4.b. In addition, since the controller has no pole at the origin, the response exhibits a steady-state error of approximately 0.91%; it is important to remark that a smaller steady-state error could be obtained by increasing the dc-gain of $W_2(s)$.

As far as noise attenuation is concerned, notice from Fig. 7 that the noise level in $i_{Sqref}(t)$ has decreased from approximately -10 to 25% for the 1-block H_∞ controller (top plot) to -5 to 6% for the 2-block H_∞ controller (bottom plot).

VI. CONCLUSION

In this paper, H_∞ optimal control has been successfully applied for speed control and noise attenuation in rotor flux oriented controlled induction motor drives. Another contribution of the paper is that the influence of the inexact knowledge of the rotor time constant on the linear model of induction motors and speed performance cannot be simultaneously considered in an H_∞ design since the former gives rise to a low pass weighting function; therefore contradicting the usual H_∞ requirement of high pass weighting function for robust stability.

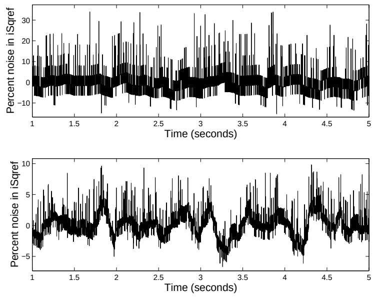

Fig. 7. Noise level in $i_{Sqref}(t)$ for 1-block (top plot) and 2-block (bottom plot) H_∞ controllers

REFERENCES

[1] W. Leonhard, *Control of Electrical Drives*, Springer-Verlag, Berlin, Germany, 2nd edition, 1996.

[2] J. A. Santisteban and R. M. Sthephan, "Vector control methods for induction machines: an overview," *IEEE Transactions on Education*, vol. 44, pp. 170–175, 2001.

[3] G. Zames and B. A. Francis, "Feedback, minimax sensitivity, and optimal robustness," *IEEE Transactions on Automatic Control*, vol. 28, pp. 585–601, 1983.

[4] B. A. Francis, "A course in H_∞ control theory," in *Lecture Notes in Control and Information Sciences*, Berlin : Germany, 1987, vol. 88, Springer-Verlag.

[5] C. Attaianese, G. Tomasso, and A. Perfetto, "Field oriented control of induction motor by means of a H_∞ controller," in *Proceedings IEEE Symposium on Industrial Electronics*, Bled : Slovenia, 1999.

[6] A. Makouf, M. E. H. Benbouzid, D. Diallo, and N. E. Bouguechal, "Induction motor robust control: an H_∞ control approach with field orientation and input-output linearizing," in *Proceedings of the '27th Annual Conference of the IEEE Industrial Electronics Society*, Denver : USA, 2001.

[7] J. C. Doyle, K. Glover, P. P. Khargonekar, and B. A. Francis, "State-space solutions to standard H_2 and H_∞ control problems," *IEEE Transactions on Automatic Control*, vol. 34, pp. 831–847, 1989.

[8] J. C. Doyle, "Advances in multivariable control," in *ONR/Honeywell Workshop*, Minneapolis : USA, 1984.

[9] D. E. Rivera, M. Morari, and S. Skogestad, "Internal model control. 4. PID controller design," *Ind. Eng. Chem. Process Design Development*, vol. 25, pp. 252–265, 1986.

[10] M. Vidyasagar, *Control System Synthesis: a factorization approach*, MIT Press, Cambridge, USA, 1985.

[11] S. J. Chapman, *Electric Machinery Fundamentals*, McGraw-Hill Inc., New York, USA, 2nd edition, 1991.

[12] K. J. Astrom and T. Haglund, *Automatic Tuning of PID controllers*, Instrument Society of America, Research Triangle Park, NC, 1st edition, 1988.

[13] J. C. Doyle, B. A. Francis, and A. Tannenbaum, *Feedback control theory*, Macmillan Publishing Company, New York, 1992.